Vol. 740: 193–211, 2024
https://doi.org/10.3354/meps14635

MARINE ECOLOGY PROGRESS SERIES
Mar Ecol Prog Ser

Published July 25

Assessing the population consequences of disturbance and climate change for the Pacific walrus

Devin L. Johnson[1,*], Joseph M. Eisaguirre[2], Rebecca L. Taylor[2], Joel L. Garlich-Miller[1]

[1]US Fish and Wildlife Service, Marine Mammals Management, 1011 E. Tudor Rd., Anchorage, AK 99503, USA
[2]US Geological Survey, Alaska Science Center, 4210 University Drive, Anchorage, AK 99508, USA

ABSTRACT: Climate change and anthropogenic disturbance are increasingly affecting wildlife at a global scale. Predicting how varying types and degrees of disturbance may interact to influence population dynamics is a key management challenge. Population consequences of disturbance (PCoD) models provide a framework to link effects of anthropogenic disturbance on an individual's behavior and physiology to population-level changes. In the present study, we develop a Pacific walrus (*Odobenus rosmarus divergens*) PCoD model to encompass the population-level effects of both anthropogenic disturbance and climate change. As the Arctic becomes increasingly ice-free, walruses spend more time at coastal (vs. ice-based) haulouts, from which they must expend more energy to reach foraging areas and where they have an elevated risk of mortality. Concurrently, sea ice loss is increasing the anthropogenic footprint in the Arctic (e.g. fisheries, shipping, energy exploration), which creates additional disturbance. We applied the PCoD model to 4 scenarios (ranging from optimistic to pessimistic) which incorporate different global sea ice model projections along with varying degrees of anthropogenic disturbance. All scenarios indicated a decline in Pacific walrus vital rates by the end of the 21st century, but our results demonstrated that the intensity of that decline could be mitigated by global efforts to reduce carbon emissions, along with local management and conservation efforts to protect important coastal haulouts and foraging grounds. In summary, we introduce a flexible PCoD modeling framework in a novel context which will prove useful to researchers studying species threatened by rapid environmental change.

KEY WORDS: Arctic · Climate change · *Odobenus rosmarus* · Pacific walrus · Population consequences of disturbance

1. INTRODUCTION

Because of changing global conditions, wildlife populations are under increasing pressure from direct and indirect anthropogenic effects that influence animal behavior on an individual basis. These behavioral changes might alter an animal's physiology and lifetime reproductive success, often with lasting population-level effects (e.g. Pirotta et al. 2019). Thus, frameworks are needed for analyzing and predicting how animals respond to disturbance and changing environmental conditions and how those responses result in population changes for species of conservation and management concern.

Population consequences of disturbance (PCoD) models (reviewed by Pirotta et al. 2018) provide a framework to link disturbance at the individual level to effects at the population level. Originally conceptualized in the context of acoustic disturbance in marine mammals (National Research Council 2005), this approach has been applied to a wide range of animal populations and has recently been adapted to include interactive effects of both disturbance and environmental change (Pirotta et al. 2019). Bioenergetic

*Corresponding author: devin_johnson@fws.gov

models are particularly useful in this framework because they can simulate individual movement and energy acquisition — and subsequent effects on body condition, survival, and reproduction (e.g. New et al. 2013). The dynamic energy budget (DEB; De Roos et al. 2009) is one such model to simulate an animal's daily body condition and lifetime reproductive success by balancing energy gain (resource assimilation) and energy loss (metabolism, growth, fetal development, and lactation). Hin et al. (2019) further integrated a DEB model for use in a PCoD framework for pilot whales *Globicephala melas*, introducing a powerful tool for simulating population consequences of disturbance and environmental change in marine mammal populations.

The Pacific walrus *Odobenus rosmarus divergens* is a large, tusked pinniped distributed across the Bering and Chukchi seas and coasts of Alaska and Russia. They are estimated to have a population of 171 000–366 000 individuals (95% credible interval [CrI]; Beatty et al. 2022) and have been an important traditional subsistence resource for local indigenous communities for millennia (MacCracken 2012). Because the Pacific walrus is an arctic–subarctic specialist that depends on sea ice for its reproductive success (i.e. as a substrate to give birth on and to rest on between foraging bouts; Fay 1982), concerns have been raised that its population may decline by the end of the 21st century (e.g. MacCracken et al. 2017). As the climate has warmed and sea ice has become less available for female Pacific walruses and their calves to rest on in the Chukchi Sea in summer and autumn, they have increasingly hauled out to rest on land (Fischbach et al. 2022), where they experience a greater risk of disturbance-based mortality (Jay et al. 2012, Udevitz et al. 2013). Additionally, they spend less time foraging and resting when sea ice is not available because of the long distance between some land-based haulouts and productive foraging areas (Jay et al. 2017). As the region becomes increasingly ice-free, human presence, development, and impacts are also likely to increase (e.g. Lavelle 2013, Melia et al. 2016, Huntington et al. 2020). Indigenous knowledge (IK) holders (i.e. members of subsistence walrus hunting communities) have raised concerns about the impacts of increasing direct anthropogenic disturbance, such as oil and gas activities, ship and air traffic, and commercial fisheries, on the Pacific walrus population (MacCracken et al. 2017; Table S1 in the Supplement at www.int-res.com/articles/suppl/m740p193_supp.pdf). Although several of these factors have been addressed individually (e.g. Udevitz et al. 2013, 2017), there is a need for a comprehensive framework that can assess the overall impact of environmental change and disturbance.

The primary objective of this study was to develop a framework for simulating the consequences of climate change and anthropogenic disturbance on the Pacific walrus population. We developed a DEB model (following Hin et al. 2019), applying walrus-specific physiological parameters when available and relying on parameter values and assumptions from other marine mammals where walrus-specific data were unavailable. By incorporating sea ice projections in a PCoD framework, we predicted population-level responses to an array of climate change and disturbance scenarios. This tool should prove useful for evaluating conservation and management options for a species in a complex, dynamic system.

2. METHODS

2.1. Overview

We developed a DEB model for the Pacific walrus based on a set of bioenergetic parameters that simulates a female walrus' energy balance and overall reproductive success (i.e. the number of female calves a female weans over the course of her lifetime). Our DEB model incorporates a spatial component, in contrast to the model presented by Hin et al. (2019), by including daily estimates of walrus movements and activity budgets (and associated energy expenditure) in response to sea ice cover. The baseline model (i.e. under contemporary sea ice conditions) was calibrated to match population-level estimates of reproductive and age-specific survival rates from the most recent available data (Taylor et al. 2018). We developed a suite of combined climate and disturbance scenarios that incorporate sea ice projections from recent global climate models, varying degrees of anthropogenic disturbance, and mitigation of mortality at coastal haulouts as well as potential changes to prey density. After we calibrated the baseline DEB model, we applied each scenario in a PCoD framework to predict the response of the Pacific walrus population to different potential conditions up to the middle and end of the 21st century.

2.2. DEB

The DEB model (e.g. De Roos et al. 2009, Hin et al. 2019) is a state-specific bioenergetic model that tracks the daily energy assimilation and expenditure of female marine mammals to ultimately estimate lifetime reproductive success. We developed a DEB

model that relies on parameter values from the Pacific walrus literature or, when these were unavailable, from the best available surrogate species, in some cases using derived values from Hin et al. (2019) (Table 1; for further details, see Text S1).

Individual females are simulated beginning from weaning age (TC_W = 2 yr) until they die, either from old age (T_{MAX} = 44 yr) or from other causes of mortality (see Section 2.2.5). We refer to animals between 2 and 44 yr of age as 'adult females' throughout the manuscript. A female can occupy one of 4 states at any given time: non-reproductive (either an adult who is neither pregnant nor lactating, or a juvenile from weaning to age of first implantation), pregnant (but not lactating), lactating (but not pregnant), and lactating and pregnant. Each state confers different

Table 1. Summary of model parameter values and their sources. Values are walrus-specific unless otherwise noted

Symbol	Units	Value	Definition	Source
Age parameters				
T_{MAX}	Days	16060	Maximum walrus age (44 yr)	Taylor et al. (2018)
T_{RMIN}	Days	1460	Minimum possible reproductive age (4 yr)	Fay (1982)
T_{RMAX}	Days	10949	Maximum reproductive age (30 yr)	Fay (1982)
T_P	Days	310	Duration of pregnancy (active gestation)	Noren et al. (2014)
TC_R	Days	450	Calf age at which female begins to reduce milk supply and the calf's foraging efficiency is 50% of an adult's foraging efficiency	Derived from data in Fay (1982)
TC_W	Days	730	Calf age at weaning (2 yr)	Noren et al. (2014)
Growth parameters				
L_0	cm	113	Length at birth	Fay (1982)
L_∞	cm	280	Maximum length	Fay (1982)
v	d^{-1}	6.85×10^{-4}	von Bertalanffy growth rate[d]	Garlich-Miller & Stewart (1999)
ω_s	kg $cm^{-1\omega e}$	1.82×10^{-4}	Structural mass–length scaling constant[d]	Garlich-Miller & Stewart (1999)
ω_e	–	2.72	Structural mass–length scaling exponent[d]	Garlich-Miller & Stewart (1999)
Metabolic parameters				
σ_G	MJ kg^{-1}	28.5	Energy cost per unit of growth in structural mass	Noren et al. (2014)
σ_M_LI	l O_2 min^{-1}	0.00101 × MASS$^{1.25}$	Metabolic rate for resting on land or ice[a]	Rode et al. (2024)
σ_M_WS	l O_2 min^{-1}	0.00245 × MASS$^{1.13}$	Metabolic rate for activity in water, swimming[a]	Borque-Espinosa et al. (2021)
σ_M_WD	l O_2 min^{-1}	0.02820 × MASS$^{0.73}$	Metabolic rate for activity in water, diving[a]	Borque-Espinosa et al. (2021)
σ_M_WR	l O_2 min^{-1}	0.00123 × MASS$^{1.22}$	Metabolic rate for activity in water, resting[a]	Borque-Espinosa et al. (2021)
φ_r	m^3 $kg^{-2/3}$ d^{-1}	1.0	Encounter rate scalar[c]	Hin et al. (2019)
Resource parameters				
R	MJ m^{-3}	4.034	Resource availability	This study (calibration parameter)
ε^+	MJ kg^{-1}	32	Anabolic reserve conversion efficiency	Udevitz et al. (2017)
ε^-	MJ kg^{-1}	32	Catabolic reserve conversion efficiency	Udevitz et al. (2017)
ρ_S	–	0.10	Starvation threshold (reserve mass/total body mass)[b]	Noren et al. (2009)
μ_S	–	0.2	Starvation mortality scalar[c]	Hin et al. (2019)
γ	–	3	Shape parameter for relationship between resource assimilation and age[c]	Hin et al. (2019)
ρ	–	0.3 or 0.39	Target body condition for normal and late pregnancy (reserve mass/total body mass).	Harwood et al. (2019), derived from Noren et al. (2014)
η	–	15	Slope of assimilation response around target body condition[c]	Hin et al. (2019)
Lactation parameters				
σ_{LF}	–	0.9	Milk production efficiency[c]	Lockyer (1993)
σ_{LC}	–	0.95	Calf's milk assimilation efficiency[c]	Lockyer (1993)
φ_L	m^3 $kg^{-2/3}$ d^{-1}	1.0	Milk energetic scalar[c]	This study (see Text S1)
ξ_m	–	–2	Shape parameter for relationship between milk provisioning and female body condition[c]	Hin et al. (2019)
ξ_C	–	0.25	Shape parameter for relationship between milk assimilation and calf age[c]	Hin et al. (2019), this study

[a]MASS refers to the individual's total mass, defined as S_t (structural mass) + F_t (reserve mass). [b]Value for Steller sea lions *Eumatopias jubatus.* [c]Value assumed in a DEB model developed for North Atlantic long-finned pilot whales *Globicephala melas.* [d]Value from a study on Atlantic walrus *Odobenus rosmarus* rather than the Pacific walrus subspecies

energy requirements depending upon the body mass of the individual and the growth stage of her fetus or calf (if applicable). The series of interrelated state-dependent equations that balance daily energy input and expenditures within the DEB model is conceptualized in Fig. 1.

2.2.1. Structural mass

In this section, we characterize Pacific walrus structural mass on each simulation day (t). Note that age t is equal to simulation day $t + 730$, because each individual female begins the simulation at 2 yr of age. Structural mass (S_t) comprises tissues such as bones and organs that cannot be catabolized for energetic needs, whereas reserve mass (F_t; i.e. blubber) is modified in the sections below pertaining to growth, metabolism, and reproduction; thus, total mass is the sum of S_t and F_t. We define an animal's body condition as the proportion of reserve mass relative to its total mass (i.e. $\rho_t = F_t / W_t$). Because we require structural mass (as opposed to total mass) for the DEB model, we were unable to directly apply documented mass growth curves (Fay 1982) and instead relied on the generalized von Bertalanffy growth equation, which provided a reasonable fit to historical, empirical data for female Pacific walruses (McLaren 1993):

$$L_t = L_\infty - (L_\infty - L_0)e^{vt} \quad (1)$$

where L_t is body length on simulation day t, L_∞ is the maximum possible length (280 cm), L_0 is the length at birth (113 cm); and v is the growth rate (0.000685 d^{-1}; Table 1). Body length was then incorporated into Eq. (2) to estimate structural mass on day t (S_t):

$$S_t = \omega_s \times L_t^{\omega_e} \quad (2)$$

where ω_s is the structural mass–length scaling constant (1.82×10^{-4} kg $cm^{-1\omega_e}$, Table 1); and ω_e is the structural mass–length scaling exponent (2.72; Table 1). We assumed that male and female calves grow at the same rate from T_0 (birth day) to TC_W (weaning day). Although walruses are sexually dimorphic, sex-specific differences in body length growth curves appear minimal, and mass–length relationships are not significantly different between sexes in the first 2 yr of life (Fay 1982, Garlich-Miller & Stewart 1999).

We assumed that fetuses grow at a constant rate from a length of 0 cm (at implantation) to L_0 (at birth) over the course of active gestation (T_P = 310 d; Table 1) (Fay 1982). We estimated the structural mass of the fetus using the same mass–length relationship that was used for females. The resulting age-specific growth curves for female and fetal walruses are displayed in Fig. S1.

2.2.2. Energy intake and assimilation

Each female walrus assimilates energy each day from feeding according to the following equation:

$$IR_t = \frac{RS_t^{2/3}\varphi_r P_{FORAGE}}{1 + e^{-\eta\left(\frac{\rho}{\rho_t} - 1\right)}} \quad (3)$$

where IR_t is the intake rate on day t (MJ d^{-1}); R is the resource availability parameter; P_{FORAGE} (the proportion of the day the walrus is foraging) is drawn from a probability distribution that varies by region and ice cover (see Section 2.3); η is the slope of the assimilation response around the target body condition (15; Table 1); ρ is the target body condition (0.3 or 0.39; Table 1); and φ_r is an encounter rate scalar (Table 1). We define R as the daily amount of metabolizable energy each female has available to it from food resources, which changes based on body condition following Eq. (3). Thus, R is a generalized metric of environmental quality that is not intended to directly reflect empirical estimates of benthic biomass (e.g. Wilt et al. 2014) but instead facilitates scaling with ice-associated activity budgets (the proportion of the day each walrus spends foraging) and model calibration. Eq. (3) assumes that individuals forage at the maximum possible efficiency when their relative body condition (ρ_t) is low (i.e. near their starvation threshold, ρ_S; Table 1) and reduce their foraging efficiency when they approach ρ based on η (following Hin et al. 2019). The value ρ is set to 0.3 during most circumstances but rises to 0.39 during the second half of pregnancy to replicate an observed increase in the reserves of pregnant females (Noren et al. 2014). Following this equation, animals are allowed to compensate for the effect of lost foraging opportunities on their relative body condition by increasing energy assimilation on subsequent days, provided sufficient resources are available (Fig. S2).

In many marine mammals, energy reserves (i.e. blubber) provide a buffer for incoming and outgoing energy flows for both the female and her calf (De Roos et al. 2009). In the model, surplus energy is converted to reserves if the assimilated energy (i.e. IR_t) exceeds total energy expenditure on a given day. Reserves are catabolized if the opposite is true. The energetic cost of creating each kg of reserve tissue is ε^+ MJ, and each kg of tissue provides ε^- MJ when catabolized (Table 1).

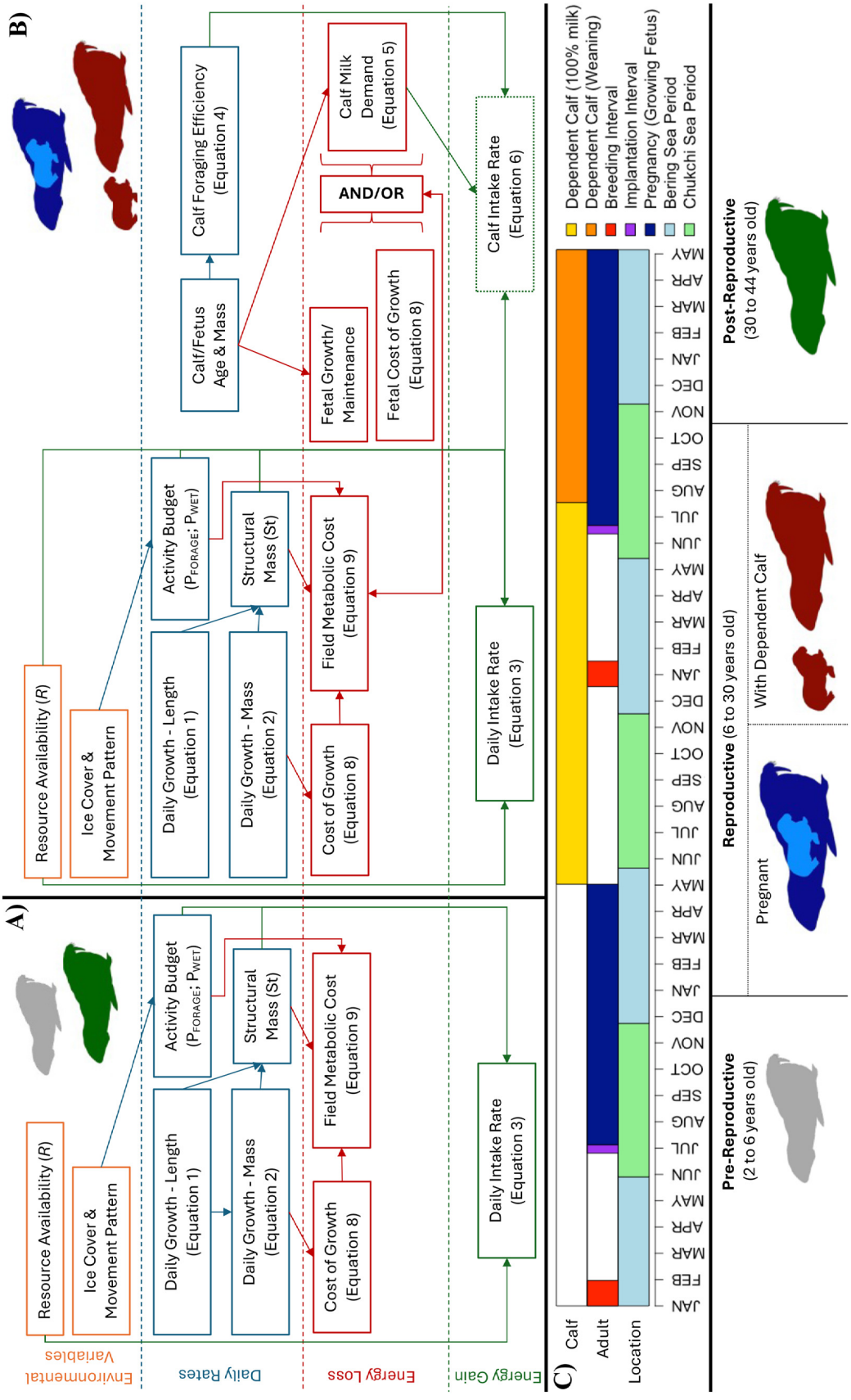

Fig. 1. Conceptual diagram of the dynamic energy budget model structure for (A) non-reproductive and (B) reproductive adult female Pacific walruses, denoting the factors contributing to daily energy balance. Some nodes in (B) depend on whether the female is pregnant, has a dependent calf, or both. A reproductive-age female who fails to implant or has a fetal or calf mortality would also be included in (A). (C) Phenology of a complete reproductive cycle of a female walrus as considered in the model (i.e. from breeding to calf independence), assuming she is able to successfully become pregnant and raise young in an optimum fashion. More detail on model parameters shown here can be found in Table 1

Walrus calves have foraging skills that are poor at birth, increase with age, and asymptote later in life (Fay 1982). We modeled this (following the relationship assumed by Hin et al. 2019) as:

$$\zeta_t = t^{\gamma} / \left(TC_R^{\gamma} + t^{\gamma}\right) \quad (4)$$

where ζ_t is foraging efficiency on day t; γ is a shape parameter quantifying the relationship between intake rate and age for individuals 0–3 yr of age (3; Table 1); and TC_R is the age at which calf foraging efficiency is 50% of adult foraging efficiency (450 d; Table 1).

Calves rely wholly or partially on milk until they are weaned (TC_W = 730 d of age) following the relationship:

$$P_{t\,\mathrm{MILK}} = \left(1 - \frac{(t - TC_R)}{(TC_W - TC_R)}\right) \Big/ \left(1 - \frac{\xi_C (t - TC_R)}{(TC_W - TC_R)}\right) \quad (5)$$

where $P_{t\,\mathrm{MILK}}$ is the proportion of a calf's milk demand that is met by the mother based on the calf's age on day t and ξ_C is a shape parameter for the relationship between milk assimilation and calf age (0.25; Table 1). $P_{t\,\mathrm{MILK}}$ is assumed to be 1 for $t < TC_R$, and 0 for $t > TC_W$, following the relationship denoted in Fig. S3.

The calf intake rate (the total amount of energy a calf obtains; Fig. S3) is derived from the following equation in a similar fashion to Eq. (3), with separate terms for assimilation from milk and foraging:

$$CI_t = \frac{RSC_t^{2/3} P_{t\,\mathrm{MILK}} \varphi_L \psi_t}{1 + e^{-\eta\left(\frac{\rho}{\rho_t} - 1\right)}} + \frac{RSC_t^{2/3} \varphi_r P_{\mathrm{FORAGE}}\, \zeta_t}{1 + e^{-\eta\left(\frac{\rho}{\rho_t} - 1\right)}} \quad (6)$$

where CI_t is the calf's energy intake rate on day t, φ_L is a scalar that reflects the difference in energy between food resources and milk (Table 1); SC_t is the calf's structural body mass at its age on Day t (Eq. 2); and ψ_t is the proportion of a calf's milk demand that is met by its mother based on the mother's starvation status (Eq. 7). Note that we effectively calibrated the model with a φ_L value of 1.0, implying that milk and food resources provide the same amount of energy per unit (see Text S1).

If the mother's body condition reaches or approaches ρ_S, she reduces the amount of milk she supplies to her calf (ψ_t; Fig. S3) following the equation:

$$\psi_t = \frac{(1 - \xi_m)(\rho_t - \rho_s)}{(\rho - \rho_s) - \xi_m (\rho_t - \rho_s)} \quad (7)$$

where ξ_m is a shape parameter (−2; Table 1); and ρ_t, ρ, and ρ_S represent the mother's body condition (current, targeted, and starvation threshold, respectively).

With these values, if the mother is in good body condition (i.e. $\rho_t \simeq 0.3$), she provides all of the calf's demands for milk during the first 14 mo of its life; milk provisioning falls monotonically to zero at weaning as the calf begins to forage for a larger percentage of its energy demand (Fig. S3). If females are in very poor condition, they will cease to provide any milk for their calves before they are weaned, often resulting in calf mortality.

The total daily energetic cost of a female's milk production can be calculated by dividing her calf's energy intake from milk on day t (the first term of Eq. 6) by the efficiency at which reserves are converted to milk (σ_{LF} = 0.9; Table 1) and the efficiency at which milk is assimilated by the calf (σ_{LC} = 0.95; Table 1). Given that simulated females under 10 yr of age have lower reserves than older females, they are more likely to have starvation-related calf mortalities, mimicking relationships observed in wild populations (Noren et al. 2014).

2.2.3. Cost of growth and metabolism

The daily cost of growth is calculated as the difference in structural mass between consecutive days, multiplied by the energy cost per unit of structural growth (σ_G = 28.5 MJ kg^{-1}; Table 1):

$$CG_t = (S_t - S_{t-1})\, \sigma_G \quad (8)$$

Along with growth, each animal's daily field metabolic cost (FM_t) is calculated based on its daily activity budget. A simulated walrus can occupy each of 4 activity states which confer different whole-body metabolic rates (Table 1): resting on land or ice (σ_M_LI); surface or subsurface swimming (σ_M_WS); diving (i.e. foraging on the ocean floor; σ_M_WD); or resting in the water (σ_M_WR; Fig. S4). Each animal spends a certain percentage of each day in the water (P_{WATER}), and a certain percentage of its in-water time actively foraging (P_{FORAGE}). When foraging, a walrus spends a certain amount of its time either diving (77.2%) or resting between dives (22.8%; mean values from Udevitz et al. 2017). We assume that when walruses are in the water and not foraging, they are either traveling to foraging grounds or migrating. From this, we can calculate an animal's whole-body metabolic rate of being in the water (σ_M_W) and calculate total daily FM_t:

$$FM_t = \left[\left(P_{\mathrm{WATER}}\, \sigma_M\_W + (1 - P_{\mathrm{WATER}})\, \sigma_M\_LI\right)\right] \times 4.8 \times 0.004184 \times 1440 \quad (9)$$

where

$$\sigma_M\_W = P_{\mathrm{FORAGE}}\, \sigma_M\_WD \times 0.772 + P_{\mathrm{FORAGE}}\, \sigma_M\_WR \times 0.228 + (1 - P_{\mathrm{FORAGE}})\, \sigma_M\_WS \quad (10)$$

Note that the following steps are taken to convert metabolic units from l O_2 min^{-1} to MJ d^{-1}: 4.8 is the conversion from l O_2 to kcal, 0.004184 is the conver-

sion from kcal to MJ, and 1440 is the conversion from minutes to days. The daily activity budget of neonatal calves (age 0–90 d) is different from that of all other walruses because they are thought to spend the majority of their time resting as they rapidly accumulate mass from their mother's milk (Fay 1982). Thus, the model applies resting metabolic rates to calves during this period. Calves > 90 d of age were assumed to have the same activity budgets as their mothers, but the metabolic rates modified the energetic costs of this activity budget based on the calf's size.

2.2.4. Reproduction

If a simulated female is over 4 yr of age (T_{RMIN}; Table 1) and her reserve mass and related body condition exceed a certain threshold ($\rho_t > 0.3$; Harwood et al. 2019) during a 10 d period starting on 1 July (mean implantation date; Fay 1982), she can become pregnant. We applied age-specific ovulation rates to each female from ages 4–9 based on published estimates (Fay 1982), ranging from 10.7% at age 4 to 100% at age 10. For each reproductive attempt, we performed a random draw incorporating these age-specific ovulation probabilities multiplied by a 90% implantation success rate to determine the probability that a female becomes pregnant (following Fay 1982). Pacific walruses are only physiologically capable of producing one calf every 2 yr due to a gestation period (passive + active) that is longer than 1 yr (Noren et al. 2014); thus, the model assumes that females cannot become pregnant during their first year of lactation. Females were given a maximum reproductive age (T_{RMAX}) of 30 yr (following Fay 1982), allowing for a 24 yr potential reproductive interval. To summarize results throughout this study, we define a 'reproductive adult' to be from 6 through 30 yr of age, although the DEB model includes the small probability that a walrus is capable of becoming pregnant at ages 4 or 5 (following Fay 1982).

During pregnancy, a female must cover the costs of fetal growth and maintenance (Eq. 8) for the fetus to survive (reviewed in McHuron et al. 2023). Thus, the mass of the growing fetus is added to the structural mass of the pregnant female, and fetal maintenance is included in her overall metabolic cost (i.e. FM_t), applying a resting metabolic rate to the fetus's body mass. On average, calf blubber was estimated to weigh 6.48 kg at birth (constituting ~11% of total body mass; based on estimated growth curves; Fay 1982), and the energy associated with creating and maintaining that additional tissue was incorporated into the cost of gestation following the fetal walrus growth curve throughout pregnancy (i.e. Fig. S1). Additional caloric requirements for pregnant females are accounted for by ρ, which rises from 0.3 to 0.39 during the second half of pregnancy (see Section 2.2.2). Provided the pregnant female's body condition stays above ρ_S, we assume that she transfers sufficient energy to her fetus for it to grow; otherwise, a starvation trial (i.e. Eq. 11 below) is conducted for the fetus to determine whether it is aborted. Additionally, fetal survival was assumed to be 95% in the absence of starvation events (following Fay 1982); thus, we applied a daily fetal survival rate of $\sqrt[334]{0.95} = 0.99985$ over the course of the pregnancy.

2.2.5. Survival

We derived an age-dependent cumulative survival curve (for survival from background mortality causes; Fig. S5) by building a piecewise function based on age-specific survival estimates from a Pacific walrus integrated population model (IPM; the most parsimonious model from Taylor et al. 2018). This curve employs 5 age classes: neonates (age 0–90 d; annual survival: 0.65); older calves (age 91–365 d; annual survival: 0.76); juveniles (age 1–5 yr; annual survival: 0.90); reproductive adults (age 6–30 yr; annual survival: 0.99); and post-reproductive adults (age 31–44 yr; annual survival: 0.55).

The age at death under baseline (good) conditions for each individual (female or calf) was set by drawing a random number between 0 and 1, and death occurred when the daily survival probability (Fig. S5) fell below this value. Any simulated individual alive according to this baseline age at death could still die due to poor body condition. Thus, the mortality rate for each simulated individual increased when its relative body condition fell below a pre-defined value of ρ_S. On each such day when $\rho_t < \rho_S$, a Bernoulli trial was undertaken to determine the individual's survival with probability ϕ_t, defined by the following equation:

$$\phi_t = e^{-\mu_s\left(\frac{\rho_S}{\rho_t} - 1\right)} \quad (11)$$

where μ_S is a scalar defining the strength of the starvation mortality relationship (0.2; Table 1).

2.2.6. Population growth rate and intrinsic rate of increase

Individuals simulated in the DEB model represent a random sample of all possible female life histories,

and their mean reproductive success and mean age of death (life expectancy) can be used to derive an estimate of population growth rate (Harwood et al. 2019).

By simulating many (e.g. 10 000) individuals, we were able to estimate population-level parameters under different environmental conditions and scenarios (Hin et al. 2019). We defined population-level lifetime reproductive success (hereafter 'reproductive success', S_r) as the mean number of female offspring (assuming a 50:50 calf sex ratio) that were successfully raised to weaning age by all simulated individuals. The annual population growth rate (λ) can then be estimated using the following equation (e.g. Turchin 2003):

$$\lambda = S_r^{1/\bar{E}} \quad (12)$$

where $\bar{E}$ is the average life expectancy in years of all simulated individuals. Given λ, we can estimate the intrinsic rate of increase ($r = \ln[\lambda]$). Finally, the maximum intrinsic rate of increase (r_{max}) is simply the rate of population increase when the population is not limited by resources. Thus, we can estimate r_{max} by effectively providing unlimited resources to the simulation (e.g. multiplying R [Eq. 3] by 10) and then calculating r (Harwood et al. 2019). We compared this method against other conventional equations for deriving r_{max} (Cortes 2016), and found that it fell within the range of those estimates (Fig. S6) and produced values we would expect based on the species' life history (e.g. Romero et al. 2017, Moore et al. 2018). Given r and r_{max}, carrying capacity (K) can be calculated using the following formula (e.g. Turchin 2003):

$$\frac{N}{K} = 1 - \left(\frac{r}{r_{max}}\right) \quad (13)$$

2.2.7. Model calibration

One benefit of the DEB modeling framework is that it involves a flexible R parameter, which can be adjusted to simulate different environmental conditions. These are the primary mechanisms through which a baseline model can be calibrated such that its output matches empirical estimates (e.g. N/K, reproductive and age-specific survival rates). Once a baseline model is produced that matches estimated population parameters, it is possible to introduce disturbance and climate change scenarios in a PCoD framework to estimate predicted changes to those population parameters.

We calibrated our default DEB model by adjusting R until N/K, reproductive rates, and age-specific survival rates matched values found in Table S2. We defined K as the point at which population size remains constant (i.e. $N_t \approx N_{t+1}$). Pacific walrus population abundance was most recently estimated in a genetic mark–recapture study (Beatty et al. 2022), at which time the population was considered near K based on an IPM that indicated the population size was constant (Taylor et al. 2018; most parsimonious model). However, this conclusion was based on extant conditions that included harvest mortality; thus, some level of population growth would be expected if harvest was reduced (MacCracken et al. 2017). In this context, we calibrated the model to an N/K value of 0.9 to account for the effect of harvest on population dynamics, and K represents the size at which the population would remain constant over time if there were no harvest. We also calibrated the DEB model to match density-dependent annual reproductive rates (the annual probability a reproductive adult female gave birth to a female calf) and calf survival rates from the IPM (Taylor et al. 2018; most parsimonious model; Fig. S7, Table S2). Note that the model was calibrated to calf survival rates in this fashion to account for differences between baseline mortality (e.g. Fig. S5) and starvation-associated mortality.

2.3. Population consequences of climate change

The primary environmental driver for climate-associated impacts on the Pacific walrus population is a reduction in sea ice availability during the summer and autumn months in the Chukchi Sea. Behavioral changes associated with recent changes to sea ice availability have already influenced walrus activity budgets and, thus, energy expenditure (Jay et al. 2017) and may also influence demographic rates (MacCracken 2012). The population consequences of climate change on Pacific walrus bioenergetics can be broken down into 3 major factors related to sea ice availability: (1) changes in movements or foraging behavior; (2) mortality at terrestrial haulouts; and (3) influences on prey density. In the PCoD model, we relate these factors to sea ice projections to the end of the 21st century from general circulation models.

2.3.1. Sea ice projections

The Intergovernmental Panel on Climate Change's sixth assessment report features a set of global climate models (Coupled Model Intercomparison Pro-

ject, CMIP6), which includes sea ice projections under 2 shared socio-economic pathways (SSP2–4.5 [ssp245] and SSP5–8.5 [ssp585]; Fox-Kemper et al. 2021). These 2 pathways are commonly used by policymakers to characterize climate change: ssp245 represents an intermediate global carbon emissions scenario, whereas ssp585 represents a high baseline scenario in which global carbon emissions continue to rise (O'Neill et al. 2016). To characterize sea ice dynamics over the Pacific walrus range to the end of the 21st century, we analyzed ice cover from a suite of 10 CMIP6 models (Table 2) over 5 regions of the Chukchi and Bering seas (following Udevitz et al. 2017; Fig. 2, Text S1). For each climate model, we considered two 10 yr time periods (mid-century: 2045–2054; end-century: 2090–2099) and 2 shared socio-economic pathways (ssp245 and ssp585; visualized in Fig. S8). We applied a sampling protocol to incorporate the variability between models, resulting in a total of 5 sea ice scenarios (SI_0–SI_4; Table 2, Fig. 2).

2.3.2. Changes in movement and foraging behavior

Pacific walruses (particularly females and juveniles) use sea ice as a preferred habitat for much of the year, which provides a safe platform to rest on during seasonal migrations and between foraging bouts (Fay 1982). When sea ice is unavailable, females and juveniles spend more energy because of the long distance between some land-based haulouts and productive foraging areas (Jay et al. 2017). Udevitz et al. (2017) developed a model (based on telemetry data) that relates changes in sea ice availability to adult female walrus movements and activity budgets in the Chukchi Sea in summer and autumn, and then used these to predict seasonal changes in body condition under different climate scenarios. We adapted the Udevitz et al. (2017) model for use in the PCoD framework (further details in Text S2).

We used both the sea-ice-driven movement and activity models from Udevitz et al. (2017) to generate Bayesian posterior predictive distributions of daily activity budgets for Pacific walruses across 5 movement pathways (Fig. 3) under the 5 different sea ice scenarios (Table 2). The samples from these distributions generated daily estimates of the following activity budget parameters: P_{WATER}, P_{FORAGE}, and the region it occupies each day (Regions 0–4; Fig. 3). These values link the daily FM_t (Eq. 9) and IR_t (Eq. 3) to ice cover and incorporate behavioral changes associated with ice availability (e.g. differential travel costs to foraging areas). Our baseline model uses sea ice estimates for contemporary conditions (i.e. SI_0; Table 2), and models incorporating sea ice projections (SI_1–SI_4) simulate the response of Pacific walrus energy intake and expenditure to ice loss.

2.3.3. Mortality at terrestrial haulouts

As summer and autumn sea ice availability in the Chukchi Sea has decreased over recent years, large numbers of walruses have used terrestrial haulouts (rather than hauling out on ice; Fischbach et al. 2009, 2022), which increases the probability of disturbance-related mortalities (Udevitz et al. 2013). Young calves are particularly susceptible to mortality at terrestrial

Table 2. The 5 sea ice scenarios used to assess walrus population consequences of climate change. Shared socio-economic pathways (SSPs) were developed by the Intergovernmental Panel on Climate Change and represent a ssp245 and a ssp585 carbon emission mitigation scenario

Name	SSP	Projection period	Ice data source
SI_0	NA	2008–2014 (contemporary)	MIZ and SIGRID-3[a]
SI_1	ssp245	2045–2054 (mid-century)	CMIP6 Suite[b]
SI_2	ssp245	2090–2099 (end-century)	CMIP6 Suite[b]
SI_3	ssp585	2045–2054 (mid-century)	CMIP6 Suite[b]
SI_4	ssp585	2090–2099 (end-century)	CMIP6 Suite[b]

[a]Historical sea ice data for the 2008–2014 period were compiled by Udevitz et al. (2017) using MIZ (Marginal Ice Zone) and SIGRID-3 (Sea Ice Grid 3) charts

[b]For each sea ice projection, we applied a sampling protocol to randomly incorporate data from the following suite of CMIP6-endorsed models (institute and host country): ACCESS-CM2 (CSIRO-ARCCSS, Australia), ACCESS-ESM1.5 (CSIRO, Australia), CanESM5 (CCCma, Canada), CESM2-WACCM (NCAR, USA), CNRM-ESM2-1 (CNRM-CERFACS, France), EC-Earth3 (EC-Earth Consortium, Europe-wide), EC-Earth3-Veg (EC-Earth Consortium, Europe-wide), IPSL-CM6A-LR (IPSL, France), MIROC6 (MIROC, Japan) and MRI-ESM2-0 (MRI, Japan)

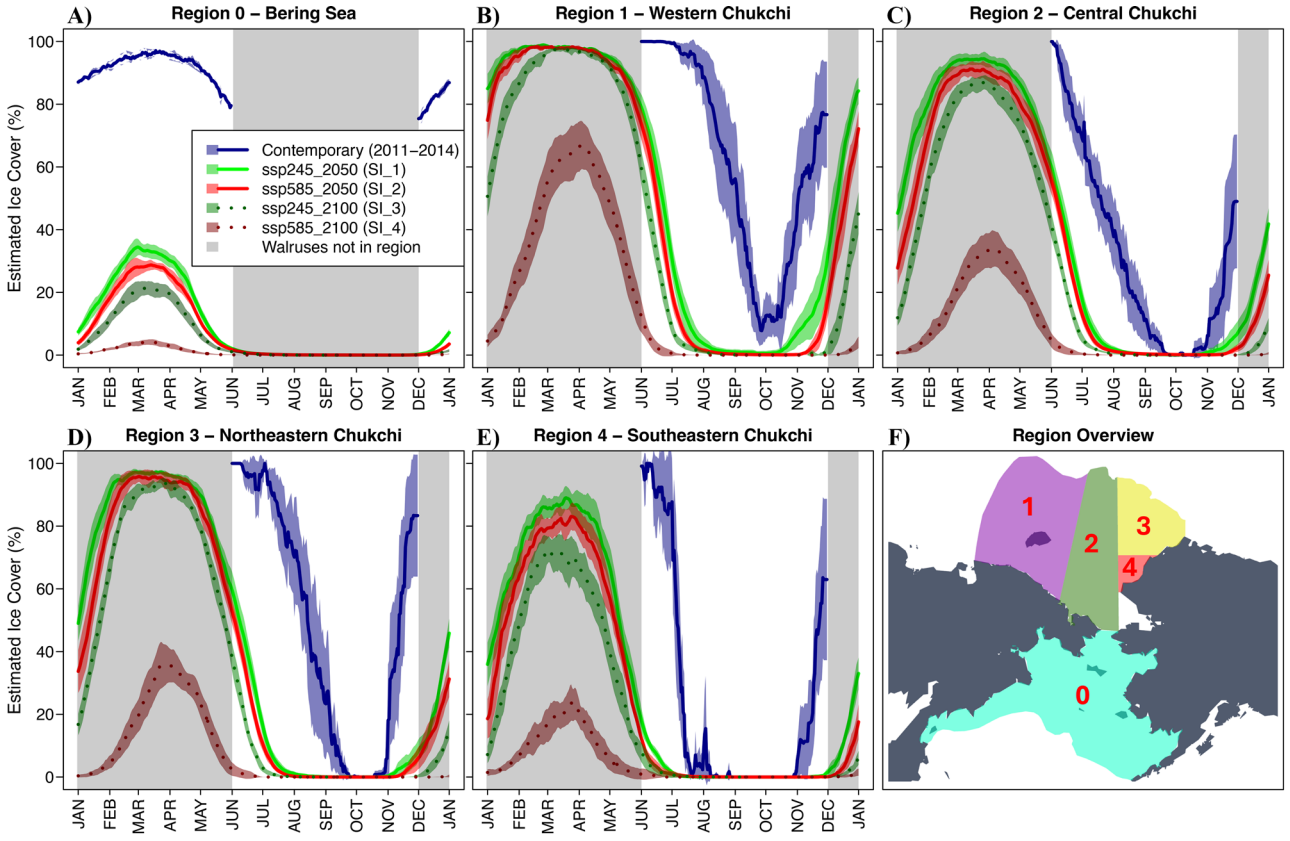

Fig. 2. Sea ice projections for the 5 regions of the study area, based on historical data (blue) and 4 climate scenarios (green, red, dark green, dark red) averaged across the suite of 10 CMIP6 climate models used in this study. For ssp245_2050 and ssp585_2050, sea ice projections include projections from 2045–2054, and for ssp245_2100 and ssp585_2100, sea ice projections include projections from 2090–2099. Lines: the mean of 10 yr of projected data for each day of the year; shaded polygons: 95% density intervals representing the variability across years and models. Gray rectangles: periods during which modeled walruses are not in their respective regions (i.e. the Chukchi Sea during the winter and the Bering Sea during the summer). Contemporary estimates of sea ice were not available for non-walrus periods

haulouts, both from predators (e.g. polar bears) and from being trampled in human disturbance-initiated stampedes (e.g. from aircraft or vessel traffic; Fischbach et al. 2009). Terrestrial haulouts on the Chukchi coast have been monitored in recent years and can be used by >150 000 individuals in some instances (Fischbach et al. 2022). Minimum annual haulout mortality estimates ranged from 20–3400 individuals between 2007 and 2016 (MacCracken et al. 2017). Pacific walrus haulout mortality may increase as a function of sea ice loss (Udevitz et al. 2013).

To account for haulout mortality in our climate scenarios, we created a terrestrial haulout day (THD) parameter which we defined with the indicator function:

$$\mathrm{THD} = 1\left\{\frac{1}{7}\sum_{d=1}^{7} \mathrm{IC}_{t-d} < 0.01\right\} \quad (14)$$

where IC is the ice cover in the simulated individual's current region. In other words, if an individual has been in a region with a mean of <1% ice cover over the past 7 d, it must rest at, and base its foraging bouts from, a terrestrial haulout. We base this estimate of 7 d on observations of walrus behavior at sea (e.g. in Fay 1982) and on preliminary analysis of satellite tracking data paired with ice availability (Fischbach & Jay 2018). Under the baseline model, an individual has an average of 37 THDs (Fig. S9), which is consistent with contemporary estimates (Fischbach & Douglas 2022). Note that each THD is simply a day a simulated walrus spends basing from a terrestrial haulout (rather than ice) and does not confer 24 h spent hauled out on land — activity budgets are calculated irrespective of whether a walrus is hauling out on land or ice (Eq. 9).

We derived daily probabilities of baseline terrestrial haulout mortality that vary based on a simulated walrus's region and whether it is a female or a calf ($\phi_{\mathrm{THM\_F}}$ and $\phi_{\mathrm{THM\_C}}$; Table S3) based on haulout mortality estimates from MacCracken et al. (2017; further details in Text S3). On each THD, we performed a Ber-

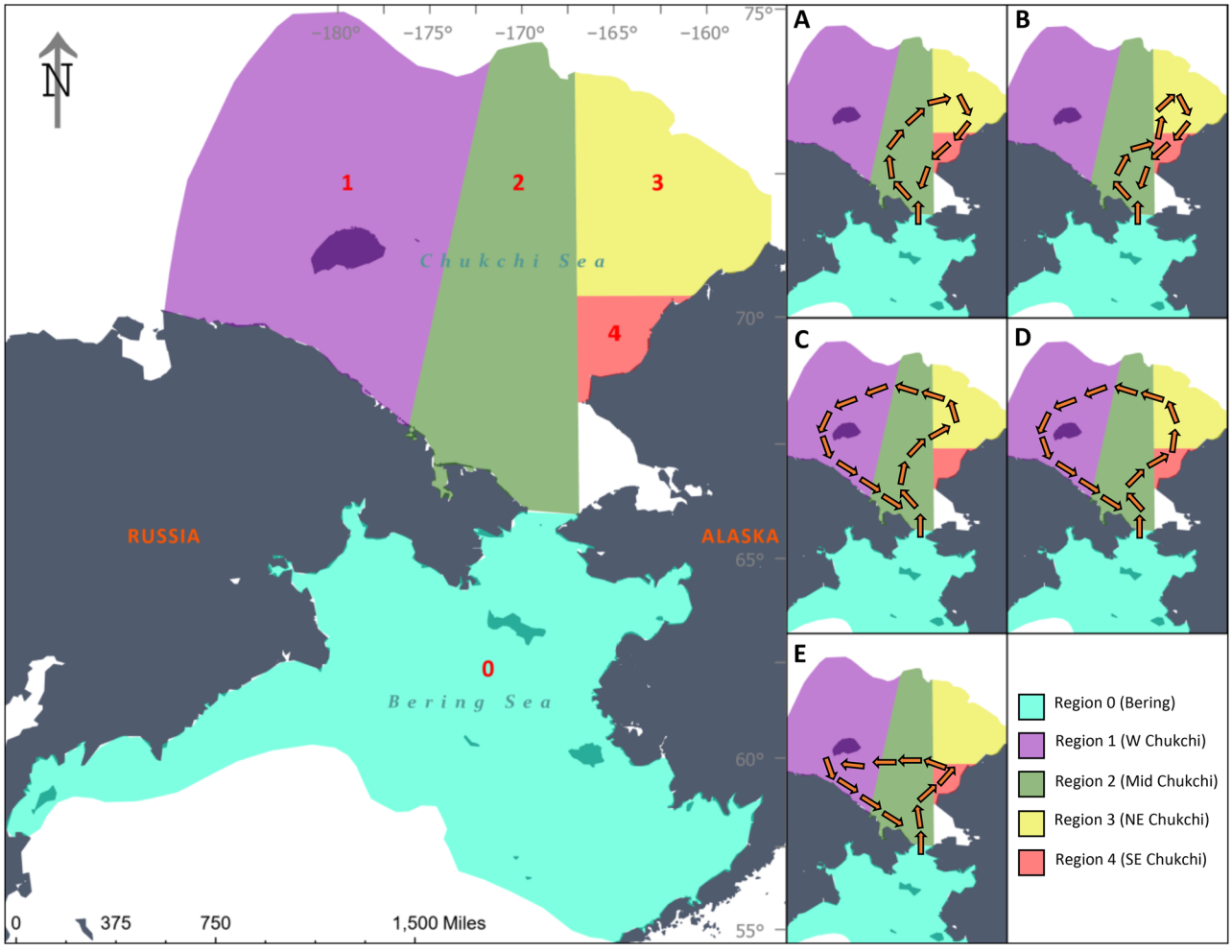

Fig. 3. Study area, denoting the annual range of the Pacific walrus divided into the 5 regions (0–4) considered in this study. The Kotzebue Sound portion of the Chukchi Sea (south of Region 4 and east of Region 2) is not walrus habitat and was not included in the study. Dark regions within shaded regions are islands. Smaller panels (A–E) represent the 5 movement pathways during the summer period in the Chukchi Sea (June–November) identified by Udevitz et al. (2017) and used in the dynamic energy budget

noulli trial with success probability ϕ_{THM_C} to determine calf survival and ϕ_{THM_F} to determine adult survival. Additionally, to represent observed stochastic 'bad years' (BYs) when larger die-offs have occurred (e.g. Fischbach et al. 2009), we similarly derived BY probabilities for females and calves ($\phi_{THM\_BY\_F}$ and $\phi_{THM\_BY\_C}$; Table S3). If a simulated walrus is determined to be experiencing a BY for terrestrial haulout mortality (formulated to occur randomly a certain number of times throughout its lifetime), BY probabilities are applied to each Bernoulli trial in that year rather than baseline probabilities.

Finally, we added a haulout mortality management (HMM) parameter to simulate the effect of management and conservation efforts on mitigating coastal haulout mortalities. Specifically, this may encompass ongoing and future agency efforts to protect coastal haulouts from aircraft (e.g. FWS 2016) and vessel traffic disturbance by establishing buffer zones around haulouts. This parameter (ranging from 0.0–1.0) is multiplied by one minus the probability of calf haulout mortality (ϕ_{THM_C}) or adult haulout mortality (ϕ_{THM_F}), ultimately reducing it. For instance, an HMM value of 0.2 would reduce the baseline haulout mortality probability by 20%, simulating management and conservation efforts such as maintaining a buffer zone around known terrestrial haulouts to reduce disturbance (e.g. Garlich-Miller et al. 2011). The probability of calf or adult haulout mortality in BYs ($\phi_{THM\_BY\_C}$ or $\phi_{THM\_BY\_F}$) was not modified by the HMM parameter to maintain the simulated stochasticity of such events.

Thus, an individual's survival in any given scenario was determined by the product of 2–4 Bernoulli trials, in the following order, to determine if the individual survived: (1) the background mortality rate based on its age at death under good conditions, (2) starvation (if applicable), (3) terrestrial haulout-based mortality (which may or may not have been mitigated by management), and (4) the effects of a bad terrestrial haulout year (if applicable).

2.3.4. Influences on prey density

Little is known about the composition and biomass of benthic invertebrates in the Chukchi Sea and how changing sea ice availability, warming subsurface sea temperatures, phytoplankton blooms (Arrigo & van Dijken 2015), and range expansions of pelagic species (e.g. Huntington et al. 2020) may ultimately influence Pacific walrus prey density (MacCracken et al. 2017). There is some evidence from focused regional studies that indicates a decline in benthic biomass in the southern Chukchi Sea (Grebmeier et al. 2015), but, by contrast, a longer ice-free interval could theoretically increase foraging opportunities, as has been postulated for Atlantic walruses *Odobenus rosmarus rosmarus* (Laidre et al. 2008). To represent changes to prey density in projected climate change scenarios, we used a parameter (PD) which proportionally weights the *R* parameter (Table 1).

2.4. PCoD

Several different types of anthropogenic disturbance may adversely impact walrus behavior (Table S1) (MacCracken et al. 2017), but little information exists on specific behavioral responses that walruses may exhibit. An expert elicitation (EE) was conducted in 2019 to generate expert opinion-based probability distributions of transfer functions from acoustic anthropogenic disturbance to Pacific walrus behavior (Harwood et al. 2019). The EE quantified the reduction of an adult female Pacific walrus' daily foraging effort in response to an acute acoustic stressor (i.e. a seismic survey) and to a continuous acoustic stressor (i.e. a drilling operation; Fig. S10).

The DEB framework uses these transfer functions to link behavioral responses to disturbance and, ultimately, to population-level effects. Daily behavioral responses that result from disturbance can be incorporated into scenarios by specifying the following parameters: disturbance type (seismic or drilling), the number of disturbance days per year, whether those disturbance days occur randomly during the June–November period or during a specified timeframe, whether disturbance occurs during consecutive days or years, the number of years in an individual's lifetime that disturbance takes place, and whether those disturbance years occur randomly or at a specified age. When a simulated walrus experiences a disturbance day, its foraging effort is adjusted based on a random draw from one of 2 distributions, depending on the disturbance type (Fig. S10). This framework allows managers the flexibility to simulate specific development projects (and their effects on different age classes), or to consider disturbance under more generalized scenarios.

2.5. Scenarios

Based on input from wildlife managers and IK stakeholder groups, we identified 4 primary climate and disturbance scenarios (which represent a broad range of potential conditions that Pacific walruses may experience in the future; Fig. 4) to demonstrate our modeling framework. Although we include and discuss these 4 scenarios, the PCoD framework is highly flexible and designed to assess a wide array of additional scenarios. Each scenario incorporates the following variables: a climate scenario (ssp245 or ssp585) and the associated effects of sea ice availability, changes to PD, the HMM factor, the number of BYs for haulout mortality, and the amount of anthropogenic disturbance (e.g. from drilling or seismic surveys). We conducted sensitivity tests to assess the individual effects of these variables on model output and ultimately to determine their relative importance in the 4 combined scenarios. In our scenarios, disturbance days occurred randomly in randomized years. Each disturbance day had a 50% chance of the disturbance being seismic versus drilling, and the simulated individual's foraging intake was modified by a random draw from the distribution associated with each disturbance type (Fig. S10). For the range of variation considered for each variable (e.g. 1–3% for the PD scalar; Fig. 4) we selected a random value for each simulated individual. For each of the 4 scenarios (optimistic, intermediate_ssp245, intermediate_ssp585, pessimistic; Fig. 4), we estimated K and r_{max} for the years 2050 and 2100, each with 100 simulations each comprising 100 individuals (i.e. 10 000 individuals total), which adequately expressed both between-individual and between-population variability (e.g. Fig. S11).

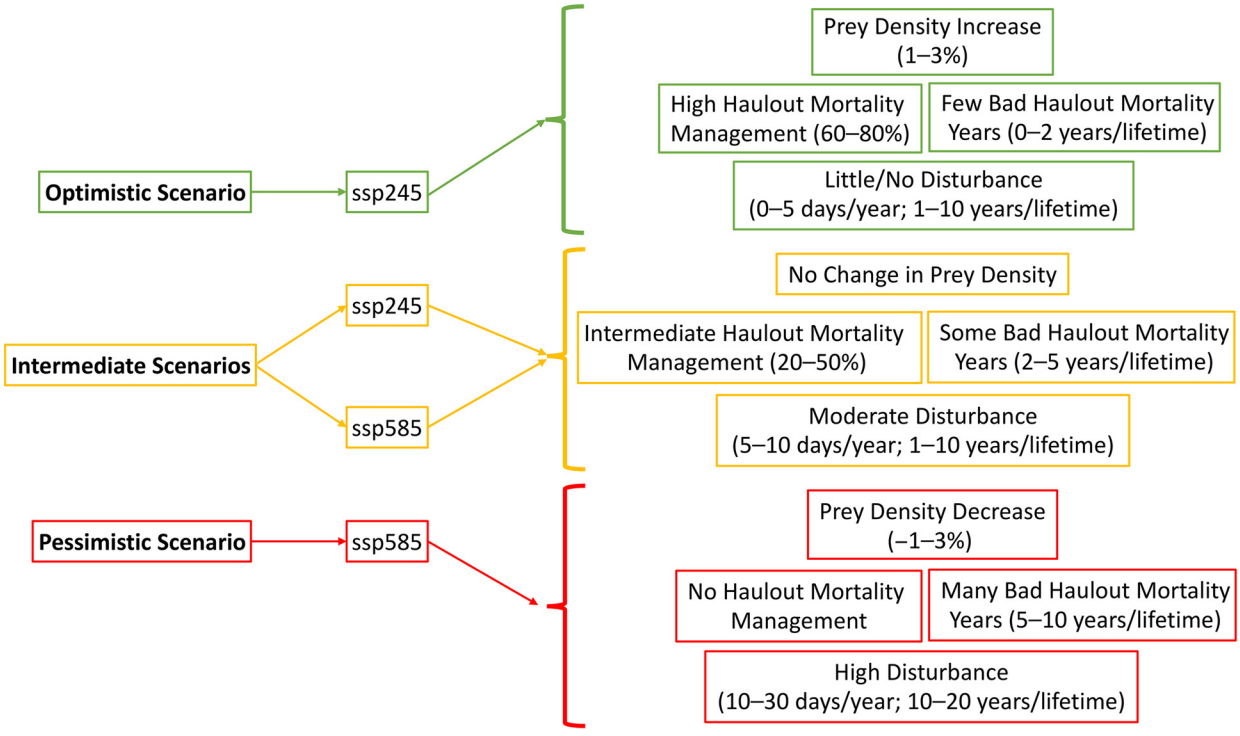

Fig. 4. Summary of climate and disturbance scenarios developed for the present study. ssp245 and ssp585 refer to Intergovernmental Panel on Climate Change CO_2 emissions scenarios and their associated sea ice projections. We refer to several displayed scenario components as acronyms throughout the manuscript: prey density (PD); haulout mortality management (HMM); bad haulout mortality year (BY)

2.6. Model sensitivity

We conducted a series of analyses to assess the model's sensitivity to several core bioenergetic parameters and scenario parameters. These included ρ, ρ_S, FM_t, φ_L, THD, PD, and anthropogenic disturbance (both days per year and years per lifetime). The range of values used in each sensitivity test appears in Table S4. Statistical significance between groups of model parameters was determined via ANOVA and post hoc Tukey tests. All analyses were conducted using the R statistical software (R Core Team 2023).

3. RESULTS

3.1. Calibration and sensitivity of DEB

The DEB was effectively calibrated to reproduce demographic rate estimates for 2015 produced with an IPM (Taylor et al. 2018; most parsimonious model; Table S2). Specifically, ≥70% of simulations that were calibrated to an R of 4.034 (n = 200 simulations each containing 100 individuals) fell within a 95% CrI of IPM estimates: 70% for reproduction, 100% for neonatal survival, and 100% for older calf survival (Fig. S7). Under these conditions, the simulated population's N/K value approximates 0.9 when ρ = 0.3 and ρ_S = 0.1 (i.e. the values in Table 1). We used the DEB model calibrated to this R under contemporary conditions (the SI_0 sea ice scenario; Table 2) to serve as the baseline model in our PCoD framework. Fig. 5 shows an example of one female walrus's simulated mass balance and reproductive success under this model, and Fig. S12 shows a simulated individual's energy balance.

The model was relatively robust to changes in ρ, whereas adjusting ρ_S or FM_t by ±10% had a significant effect on calf and adult starvation, and ultimately reproductive success (Fig. S13). The model was also relatively robust to changes in φ_L, requiring a change in ±25% to have a significant impact on reproductive success (Fig. S13).

3.2. Sea ice projections

CMIP6 sea ice projections indicated significant declines in ice cover across the 5 study regions in all 4

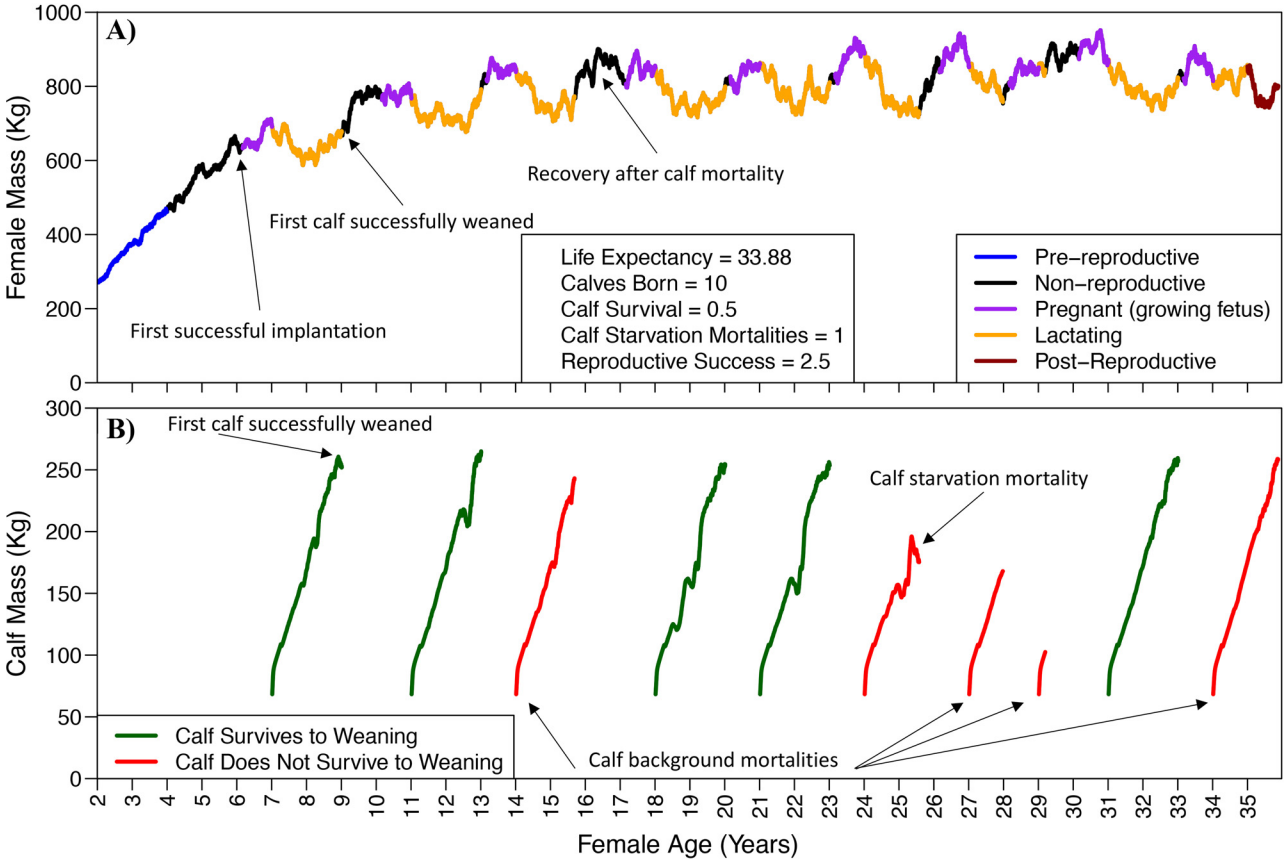

Fig. 5. Example output for one simulated female Pacific walrus over the course of the simulation. (A) Fluctuations in female body mass associated with different activity states; and (B) concurrent reproductive attempts over the female's lifetime. Reproductive success refers to the total number of female calves this walrus successfully weaned during her lifetime (total calves / 2)

scenarios (Fig. 2). Generally, this corresponds to a months-long ice-free interval across all Chukchi Sea regions during the summer and autumn months, and reduced sea ice availability during the traditional walrus breeding season in the Bering Sea. Most notably, the ssp585 sea ice scenario suggests that the traditional annual range of the Pacific walrus will be almost entirely ice-free by the end of the 21st century (Fig. 2).

3.3. Walrus response to climate-induced changes

Simulated walruses had higher energy expenditure with reduced ice cover in all climate scenarios, which resulted from their need to spend a higher proportion of time active in the water (Udevitz et al. 2017). With all other factors held constant in the model, this sea ice-induced increase in energy expenditure significantly impacted starvation-related mortality rates and reproductive success. Specifically, populations modeled under the SI_1, SI_2, and SI_3 scenarios had significantly higher rates of both adult and calf starvation, and lower calf survival (probability of the calf surviving to weaning at 2 yr old) and reproductive success than the SI_0 (baseline) scenario (Fig. S14). The SI_4 scenario (representing the ssp585 climate scenario at the end of the 21st century) exhibited the highest rates of adult and calf starvation and the lowest rates of reproductive success and calf survival (Fig. S14).

Similarly, the probability that a simulated walrus used a terrestrial haulout increased above the 2015 mean of 37 THDs under all climate scenarios. Under the ssp585 scenario, walruses experienced a mean of 96 THDs in 2050 and 248 THDs in 2100 (Fig. S9). When projecting forward to 2100, we predicted a higher proportion of THDs in the Russian Chukchi Sea and the Bering Sea than in the Alaskan Chukchi Sea, suggesting that the regional distribution of terrestrial haulouts will also change. Increased time at terrestrial haulouts created an additional source of calf and adult mortality in our climate scenarios which contributed to the decline in reproductive success (Fig. S15). The model was relatively sensitive to

BYs for terrestrial haulout mortality. Adding BYs significantly increased both calf and adult haulout mortality in an incremental fashion, which contributed to a significant decline in reproductive success when each simulated individual was subjected to 20 bad haulout years in her lifetime (Fig. S15).

The DEB model was highly sensitive to the PD scaling parameter that scaled *R*. Although a baseline DEB model calibrated to an *R* of 4.034 produced demographic rates consistent with empirical estimates for the population (e.g. Fig. S7), adjusting that *R* by ±1–5% had large impacts on starvation rates and reproductive success (Fig. S16).

Finally, we conducted an analysis to assess the effect of sea ice scenarios on the 5 walrus movement patterns (A–E). We found significant differences in adult and calf starvation, calf survival, and reproductive success between the movement patterns (Fig. S17). Specifically, movement pattern A (one of 2 patterns confined to the eastern Chukchi Sea) conferred the lowest instances of starvation and highest calf survival and reproductive success, whereas movement pattern E (one of 3 patterns using the eastern and western Chukchi Sea, but with the least northerly extent) conferred the highest instances of starvation and lowest calf survival and reproductive success; the other 3 movement patterns fell between the 2. These differences remained relatively consistent regardless of which sea ice scenario was applied (Fig. S17).

3.4. Walrus response to anthropogenic disturbance

Simulated walrus demographic rates were moderately sensitive to anthropogenic disturbance. When seismic or drilling disturbance occurred at random days during the year on 5 or 10 random years over a simulated walrus' lifetime, an extremely large number of disturbance days (i.e. 30) per year was required to significantly impact calf or adult starvation rates and associated reproductive success (Fig. S18). Exposure to 10 disturbance days for 20 yr per lifetime was enough to significantly reduce reproductive success, and the most extreme disturbance scenario (30 d yr^{-1} for 20 yr $lifetime^{-1}$) reduced overall reproductive success by 45% (Fig. S18). Although we considered anthropogenic disturbance in a randomized fashion in the present analyses, disturbance may realistically have a greater impact on starvation rates and reproductive success if it occurs (1) on consecutive days or years; (2) in a localized critical habitat area (e.g. an important seasonal foraging ground); or (3) during a time of year when walruses are more vulnerable (e.g. just after calving).

3.5. Combined climate and disturbance scenarios

The 4 primary scenarios combining climate change and disturbance (Fig. 4) all indicated declines to both Pacific walrus *K* and r_{max} by the end of the 21st century, and sooner in most cases (Fig. 6). Note that although we report estimates of *K* and r_{max} independently, the 2 are related following Eq. (13). Under the most optimistic scenario, *K* underwent a gradual decline (95% CrI for 2015: 115 019–122 066; for 2100: 102 258–108 656), as did r_{max} (95% CrI for 2015: 0.038–0.039; for 2100: 0.035–0.036). The intermediate_245 model resulted in a slightly stronger decline in r_{max} than the optimistic scenario (95% CrI for 2100: 0.032–0.033) and a larger, quicker decline in *K* (95% CrI for 2100: 72 432–75 745). The intermediate_585 model resulted in a stronger decline in *K* than the intermediate_245 model (95% CrI for 2100: 59 056–61 638), matched with a stronger decline in r_{max} (95% CrI for 2100: 0.030–0.031). Finally, our pessimistic scenario indicated severe declines to both *K* (95% CrI for 2100: 39 915–41 685) and r_{max} (95% CrI for 2100: 0.026–0.027; Fig. 6). Ultimately, this pessimistic scenario would amount to a 66% decline in *K* and a 31% decline in r_{max} by the end of the 21st century.

4. DISCUSSION

The PCoD model provided a useful framework to analyze consequences for the Pacific walrus population of climate change-induced sea ice loss—a well-recognized and growing concern among the scientific community (e.g. MacCracken 2012, Fischbach et al. 2022), Indigenous communities that rely on walruses for subsistence, and the general public. The model allows for direct and indirect effects of sea ice loss on individual behavior to be translated into changes in population demography and size. A central strength of our PCoD model is that it can incorporate new information as it becomes available, and scenarios can be tailored to evaluate the stressors of greatest concern.

We evaluated 4 example scenarios (Fig. 4), all of which resulted in a statistical decline in both *K* and the r_{max} and, thus, overall abundance and population growth rate to the end of the 21st century. Projected changes to the population were primarily driven by the rate of sea ice loss, mortality at terrestrial haul-

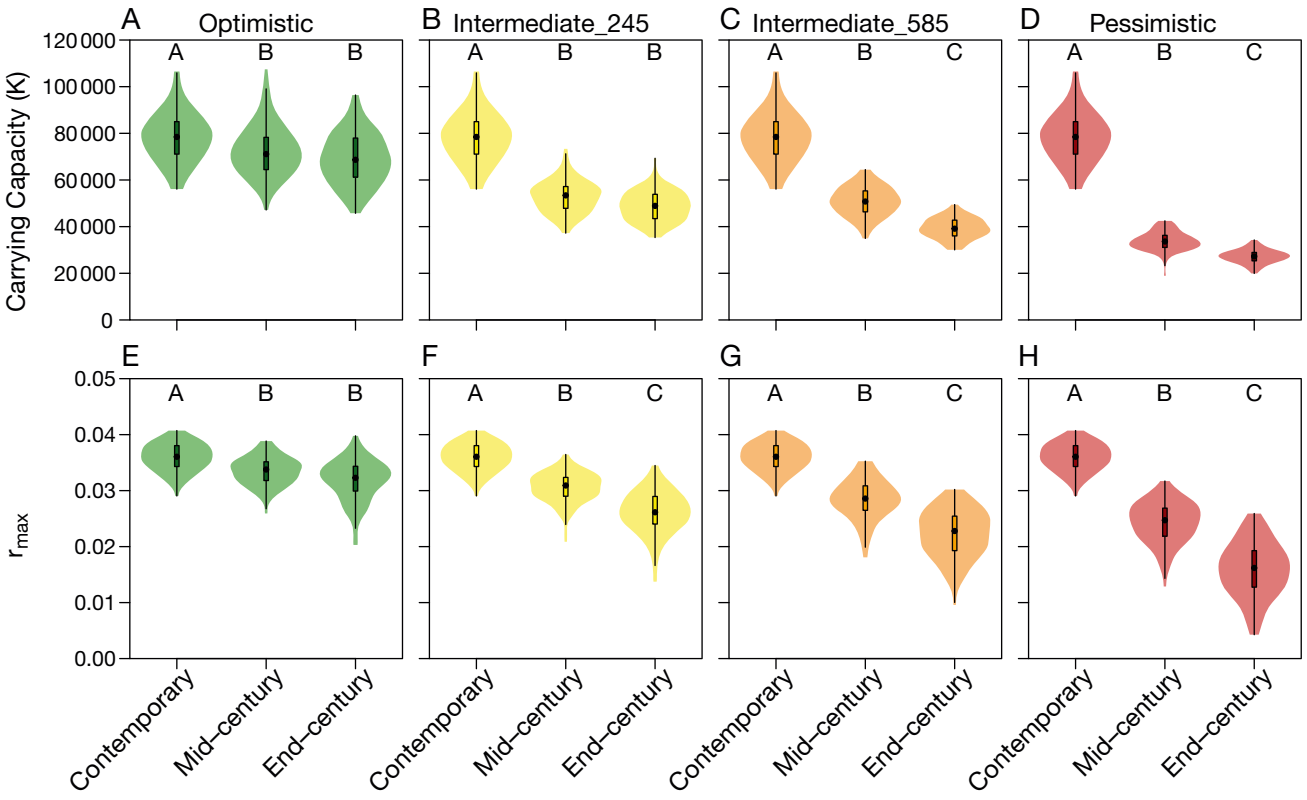

Fig. 6. (A–D) Projected carrying capacity and (E–H) intrinsic maximum rate of population growth (r_{max}) estimates for the adult female Pacific walrus population to the middle and end of the 21st century under 4 combined disturbance and climate change scenarios in the population consequences of disturbance framework (described in Fig. 4). Contemporary estimates incorporate sea ice conditions between 2008 and 2015, mid-century estimates (2045–2054), and end-century estimates (2090–2099). Different letters indicate significant differences between groups ($\alpha = 0.05$) from an ANOVA and post hoc Tukey test

outs, and changes to PD. Diminishing sea ice resulted in walruses swimming more and foraging less, thus increasing energy expenditure and decreasing energy intake. This increased adult and calf starvation rates and reduced reproductive success and calf survival (Fig. S14), which, in turn, drove the decrease in *K* (Fig. 6). Reduced PD and increased anthropogenic disturbance similarly decreased the daily walrus energy intake rate, reducing *K*. The DEB model was highly sensitive to PD and relatively sensitive to anthropogenic disturbance. Our variables associated with terrestrial haulout mortality (the number of bad haulout years and the strength of the haulout management effect) were modeled independently of *R* (i.e. they were non-density dependent) and were thus the primary drivers of the observed trends in r_{max}. Although sea ice loss was the primary driver of simulated declines in the Pacific walrus population, our results indicate that the frequency and intensity of anthropogenic disturbance (particularly at haulouts) and factors influencing PD could all have significant population effects in the future (Figs. S15, S16 & S18). Thus, our results also suggest that efforts to protect important coastal haulouts and walrus foraging grounds may be key conservation and management measures.

Movement patterns are a critical aspect of our model, and these patterns were based on data from telemetered walruses and the timing of their movements among regions relative to the amount of regional sea ice (Udevitz et al. 2017). We note, however, that the overwhelming majority of animals tracked by Udevitz et al. (2017) were satellite-tagged in the US portion of the Chukchi Sea, and, in the absence of any additional information, we assumed these movement patterns (Fig. 3) represented all major movement patterns exhibited by the population and that each pattern was equally likely (i.e. each had a 1/5 probability of being assigned to an individual). We also assumed the direction of these movement patterns will remain consistent up to the end of the 21st century. Despite these limitations, the strength of our movement pattern modeling is that residence within any given region in any movement pattern is linked to the amount of sea ice in that region; thus, our model accounts for a shift in

migratory phenology as a result of sea ice loss (Udevitz et al. 2017). Furthermore, if new telemetry data is collected, it could easily be incorporated into our modeling framework.

Although our PCoD framework has the capacity to incorporate many of the previously identified potential stressors to the Pacific walrus population (i.e. Table S1), further study is required to encompass the full suite of possible stressors associated with climate change and anthropogenic disturbance. For example, the impacts of Bering Sea ice loss on breeding and birthing platforms may have ramifications on reproductive success that are not accounted for in the model due to a lack of empirical data. Pacific walruses are thought to require sea ice platforms to breed from and give birth on (MacCracken et al. 2017); therefore, if an ice-free Bering Sea (e.g. in the ssp585 scenario) did not result in a range shift (e.g. a shift northward to sea ice refugia resulting in year-round residence in the Chukchi Sea; MacCracken 2012), our model does not account for the potential shift from breeding from and birthing on ice to breeding from and birthing on land, which could result in large reductions in reproductive success. Similarly, adult female walruses are not known to leave their calves on land and forage alone at sea (as do sea lions and fur seals, Family Otariidae); thus, we assumed that walrus calves are able to accompany their mothers everywhere and that they have the in-water endurance to do so in an ice-free environment. Although many future behavioral responses of the walrus population to climate change are unknown, a strength of the PCoD approach is the ability to explore a wide array of hypothetical scenarios (e.g. different movement patterns, shifts in breeding, or mother–calf behavior). In addition, further information is needed on the effects of climate change on the benthic community (and how that relates to future walrus PD; but see Wilt et al. 2014, Grebmeier et al. 2015) and the prevalence of harmful algal blooms and other diseases and parasites. An EE comprised of agency walrus biologists produced the probabilities that our PCoD model used to quantify walrus responses to seismic and drilling disturbance (Fig. S10; Harwood et al. 2019). An additional EE (that includes IK stakeholders) could prove beneficial for acquiring similar expert opinions for other disturbance types (e.g. ship and air traffic, fisheries, and military exercises) as well as for filling additional knowledge gaps with regards to Pacific walrus physiological and behavioral ecology.

Most bioenergetic models are, by necessity, simplifications of extremely complex natural processes. Our DEB model is based on relationships among parameters that incorporate empirical values from Pacific and Atlantic walruses, assumed values and relationships based on walrus life history, and data or assumptions from other marine mammals where walrus-specific data were not available (Table 1). For instance, we applied a starvation threshold from a study on Steller sea lions *Eumetopias jubatus* (Noren et al. 2009), and several of our scaling and shape parameters were drawn from the DEB model presented by Hin et al. (2019), who chose them to best reflect assumed biological relationships for long-finned pilot whales. As such, we have identified several data gaps in the Pacific walrus and marine mammal bioenergetic literature that were filled with assumed values in the present model. Key research needs related to Pacific walrus physiology include activity-associated metabolic rates for growing calves, further research on walrus diet and PD in the Bering and Chukchi seas, and a more robust characterization of assimilation efficiency, true metabolizable energy, and the heat increment of feeding (e.g. Booth et al. 2023). Despite the necessary assumptions we have made within this modeling framework regarding bioenergetics, its strength lies in its flexibility to compare and contrast different parameter values and projected environmental conditions.

The PCoD model we present is a flexible framework that should prove useful to wildlife managers and stakeholders to project and assess walrus population dynamics under a range of potential future conditions. In addition, while current subsistence harvest rates are thought to be sustainable (FWS 2023), a formal harvest sustainability assessment has not yet been conducted for the population (MacCracken et al. 2017) but is an active area of research. Estimates of K and r_{max} attained from our PCoD model could be used to form a baseline for a harvest sustainability assessment that can project the sustainability of different harvest scenarios to the end of the 21st century. Finally, the framework we have developed could be readily adapted to other situations and species in complex and dynamic systems and could be particularly useful for the many species simultaneously threatened by climate change and anthropogenic disturbance.

Data availability. All data and novel code used in this analysis are available at an external repository via https://figshare.com/s/cfed869a283dc4829382.

Acknowledgements. We are extremely thankful to members of the Pacific Walrus Harvest Model Steering Committee and the Eskimo Walrus Commission for their support and discussion in the development of this modeling framework:

Charles Brower, Vera Metcalf, Jacob Martin, Bryan Rookuk Jr., and Enoch Oktollik. We are also grateful to John Harwood and Cormac Booth for developing an interim Pacific walrus DEB model upon which this analysis is based. Erik Anderson, Jen Cate, and Patrick Lemons provided useful input on model development, and William Beatty and Karyn Rode provided thoughtful reviews on a previous version of the manuscript. The findings and conclusions in this article are those of the authors and do not necessarily represent the views of the US Fish and Wildlife Service. This product paper has been peer-reviewed and approved for publication consistent with USGS Fundamental Science Practices (https://pubs.usgs.gov/circ/1367/). Any use of trade, firm or product names is for descriptive purposes only and does not imply endorsement by the US Government. A pre-print of this work is available at https://doi.org/10.1101/2023.10.12.562073.

LITERATURE CITED

Arrigo KR, van Dijken GL (2015) Continued increases in Arctic Ocean primary productivity. Prog Oceanogr 136:60–70

Beatty WS, Lemons PR, Everett JP, Lewis CJ and others (2022) Estimating Pacific walrus abundance and survival with multievent mark–recapture models. Mar Ecol Prog Ser 697:167–182

Booth CG, Gulilpin M, Darias-O'Hara A, Ransijn JM and others (2023) Estimating energetic intake for marine mammal bioenergetic models. Conserv Physiol 11: coac083

Borque-Espinosa A, Rode KD, Ferrero-Fernandez D, Forte A, Capaccioni-Azzati R, Fahlman A (2021) Subsurface swimming and stationary diving are metabolically cheap in adult Pacific walruses (*Odobenus rosmarus divergens*). J Exp Biol 224:jeb242993

Cortes E (2016) Perspectives on the intrinsic rate of population growth. Methods Ecol Evol 7:1136–1145

De Roos AM, Galic N, Heesterbeek H (2009) How resource competition shapes individual life history for non-plastic growth: ungulates in seasonal food environments. Ecology 90:945–960

Fay FH (1982) Ecology and biology of the Pacific walrus, *Odobenus rosmarus divergens* Illiger. North American Fauna No. 74. United States Fish and Wildlife Service, Washington, DC

Fischbach AS, Douglas DC (2022) Pacific Walrus coastal haulout occurrences interpreted from satellite imagery (ver. 2.0, December 2022). US Geological Survey data release. https://doi.org/10.5066/P9CSM0KN

Fischbach AS, Jay CV (2018) Pacific walrus seasonal distribution from USGS tracking data, Chukchi and Bering seas, 1987–2015: US Geological Survey data release. https://doi.org/10.5066/F7VH5N43

Fischbach AS, Monson DH, Jay CV (2009) Enumeration of Pacific walrus carcasses on beaches of the Chukchi Sea in Alaska following a mortality event, September 2009. US Geological Survey Open File Report 2009–129. US Department of the Interior, Reston, VA

Fischbach AS, Taylor RL, Jay CV (2022) Regional walrus abundance estimate in the United States Chukchi Sea in autumn. J Wildl Manag 86:e22256

Fox-Kemper B, Hewitt HT, Xiao C, Aðalgeirsdóttir G and others (2021) Ocean, cryosphere and sea level change. In: Climate change 2021: the physical science basis. Contribution of Working Group I to the Sixth Assessment Report of the Intergovernmental Panel on Climate Change. Cambridge University Press, Cambridge, p 1211–1362

FWS (US Fish and Wildlife Service) (2016) Approach and viewing guidelines to avoid walrus haulout disturbances. US Fish and Wildlife Service, Marine Mammals Management, Anchorage, AK. https://www.fws.gov/walrus-approach-viewing-guidelines#:~:text=If%20weather%20or%20aircraft%20safety,to%20avoid%20causing%20a%20disturbance

FWS (2023) Pacific walrus (*Odobenus rosmarus divergens*): Alaska stock. US Fish and Wildlife Service, Marine Mammals Management, Anchorage, AK

Garlich-Miller JL, Stewart REA (1999) Female reproductive patterns and fetal growth of Atlantic walruses (*Odobenus rosmarus rosmarus*) in Foxe Basin, Northwest Territories, Canada. Mar Mamm Sci 15:179–191

Garlich-Miller J, Neakok W, Stimmelmayr R (2011) Field report: walrus carcass survey, Point Lay, Alaska, September 11–15, 2011. US Fish and Wildlife Service, Marine Mammals Management, Anchorage, AK

Grebmeier JM, Bluhm BA, Cooper LW, Denisenko SG, Iken K, Kedra M, Serratos C (2015) Time-series benthic community composition and biomass and associated environmental characteristics in the Chukchi Sea during the RUSALCA 2004–2012 Program. Oceanography 28: 116–133

Harwood J, Booth CG, Tollit DJ (2019) Walrus interim PCoD model: workshop report. New transfer functions for the effects of acoustic disturbance on vital rates in Pacific walrus. Report SMRUC-FWS-2019-04. US Fish and Wildlife Service, Anchorage, AK

Hin V, Harwood J, De Roos AM (2019) Bio-energetic modeling of medium-sized cetaceans shows high sensitivity to disturbance in seasons of low resource supply. Ecol Appl 29:e01903

Huntington HP, Danielson SL, Wiese FK, Baker M and others (2020) Evidence suggests potential transformation of the Pacific Arctic ecosystem is underway. Nat Clim Chang 10:342–348

Jay CV, Fischbach AS, Kochnev A (2012) Walrus areas of use in the Chukchi Sea during sparse sea ice cover. Mar Ecol Prog Ser 468:1–13

Jay CV, Taylor RL, Fischbach AS, Udevitz MS, Beatty WS (2017) Walrus haul-out and in water activity levels relative to sea ice availability in the Chukchi Sea. J Mammal 98:386–396

Laidre KL, Stirling I, Lowry LF, Wiig O, Heide-Jorgensen MP, Ferguson SH (2008) Quantifying the sensitivity of Arctic marine mammals to climate-induced habitat change. Ecol Appl 18:S97–S125

Lavelle M (2013) Arctic shipping soars, led by Russia and lured by energy. National Geographic Society, Washington, DC

Lockyer CH (1993) Seasonal changes in body fat condition of northeast Atlantic pilot whales, and their biological significance. Rep Int Whal Comm Spec Issue 14:325–350

MacCracken JG (2012) Pacific walrus and climate change: observations and predictions. Ecol Evol 2:2072–2090

MacCracken JG, Beatty WS, Garlich-Miller JL, Kissling ML, Snyder JA (2017) Final species status assessment or the Pacific walrus (*Odobenus rosmarus divergens*), May 2017 (version 1.0). Technical report. US Fish and Wildlife Service, Marine Mammals Management, Anchorage, AK

McHuron EA, Adamczak S, Costa DP, Booth C (2023) Esti-

mating reproductive costs in marine mammal bioenergetic models: a review of current knowledge and data availability. Conserv Physiol 11:coac080

McLaren IA (1993) Growth in pinnipeds. Biol Rev Camb Philos Soc 68:1–79

Melia N, Haines KE, Hawkins E (2016) Sea ice decline and 21st century trans-Arctic shipping routes. Geophys Res Lett 43:9720–9728

Moore JE, Martin AR, da Silva VMF (2018) Intrinsic growth (r_{max}) and generation time (T) estimates for *Inia geoffrensis*, in support of an IUCN Red List re-assessment. NOAA Tech Memo NMFS-SWFSC-596

National Research Council (2005) Marine mammal populations and ocean noise: determining when noise causes biologically significant effects. The National Academies Press, Washington, DC

New LF, Harwood J, Thomas L, Donovan C, Clark JS, Hastie G, Lusseau D (2013) Modeling the biological significance of behavioral change in coastal bottlenose dolphins in response to disturbance. Funct Ecol 27:314–322

Noren DP, Rea LD, Loughlin TR (2009) A model to predict fasting capacities and utilization of body energy stores in weaned Steller sea lions (*Eumetopias jubatus*) during periods of reduced prey availability. Can J Zool 87: 852–864

Noren SR, Udevitz MS, Jay CV (2014) Energy demands for maintenance, growth, pregnancy, and lactation of female Pacific walruses. Physiol Biochem Zool 87:837–854

O'Neill BC, Tebaldi C, van Vuuren DP, Eyring V and others (2016) The Scenario Model Intercomparison Project (ScenarioMIP) for CMIP6. Geosci Model Dev 9: 3461–3482

Pirotta E, Booth CG, Costa DP, Fleishman E and others (2018) Understanding the population consequences of disturbance. Ecol Evol 8:9934–9946

Pirotta E, Mange M, Costa DP, Goldbogen J and others (2019) Anthropogenic disturbance in a changing environment: modelling lifetime reproductive success to predict the consequences of multiple stressors on a migratory population. Oikos 128:1340–1357

R Core Team (2023) R: a language and environment for statistical computing. R Foundation for Statistical Computing, Vienna

Rode KD, Rocabert J, Borque-Espinosa A, Ferrero-Fernandez D, Fahlman A (2024) Effects of feeding and habitat on resting metabolic rates of the Pacific walrus. Mar Mamm Sci 40:184–195

Romero MA, Grandi MF, Koen-Alonso M, Svendsen G and others (2017) Analysing the natural population growth of a large marine mammal after a depletive harvest. Sci Rep 7:5271

Taylor RL, Udevitz MS, Jay CV, Citta JJ, Quakenbush LT, Lemons PR, Snyder JA (2018) Demography of the Pacific walrus (*Odobenus rosmarus divergens*) in a changing Arctic. Mar Mamm Sci 34:54–86

Turchin P (2003) Complex population dynamics: a theoretical/empirical synthesis. Monographs in Population Biology, Vol 35. Princeton University Press, Princeton, NJ

Udevitz MS, Taylor RL, Garlich-Miller JL, Quakenbush LT, Snyder JA (2013) Potential population-level effects of increased haulout-related mortality of Pacific walrus calves. Polar Biol 36:291–298

Udevitz MS, Jay CV, Taylor RL, Fischbach AS, Beatty WS, Noren SR (2017) Forecasting consequences of changing sea ice availability for Pacific walruses. Ecosphere 8: e02014

Wilt LM, Grebmeier JM, Miller TJ, Cooper LW (2014) Caloric content of Chukchi Sea benthic invertebrates: modeling spatial and environmental variation. Deep Sea Res II 102:97–106

Editorial responsibility: Lisa T. Ballance, Newport, Oregon, USA
Reviewed by: 3 anonymous referees

Submitted: November 7, 2023
Accepted: June 4, 2024
Proofs received from author(s): July 16, 2024